

# A rectilinear droplet stream study : Influence of lateral interaction on droplet dynamical behavior

**Atthasit A., Biscos Y., Lavergne G.**

ONERA-DMAE, Centre de Toulouse, BP 4025,  
31055 Toulouse Cedex FRANCE  
Tel:+33 0562252835 : FAX:+33 0562252583  
E-mail: anurak.atthasit@supaero.fr

The objective of this study is to determine the evolution of the droplet drag coefficient in a case of dense two phase flows. A droplet stream is surrounded with another three streams arranged in equilateral triangle arrays. The distance between the central stream and the lateral streams varies from 2 to 26 times of droplets diameter and the Reynolds number is ranging from 15 to 95.

Under low interaction between lateral droplet stream, the drag coefficient normally decreases when the droplet is under the influence of the front wake generated by the upstream droplet. For several closed adjacent streams, however, the repulsive forces between particles cause an increasing drag coefficient which can be higher than the droplet isolated case.

## 1. Introduction

Basic experiments and associated techniques are developed at ONERA/Toulouse to improve the understanding of physical phenomena occurring in the sprays in order to elaborate models for two phase flow numerical simulation. Research is now based on optimising the injection system used in the combustion chambers in the frame of the reduction of pollutant emissions of turbojets.

Dense sprays are presented in most of the applications in practical systems. It is well known that droplets in a stream do not follow the isolated droplet characteristics such as drag coefficient and size reduction for combustion state. This paper presents results obtained on monodisperse droplet streams under non-reacting conditions. The results will be presented in terms of the evolution of the droplet drag coefficient in function of the distance between droplets.

### *1.1. Droplet drag coefficient*

The drag coefficient  $C_d$  is estimated experimentally from the equation of motion for a spherical droplet. In this case, the equation can be simplified by neglecting the terms of pressure gradient and history:

$$Cd = \frac{4\rho_l D_l \left( \frac{d\vec{V}_l}{dt} - \vec{g} \right)}{3\rho_{gas} \left\| \vec{V}_{gas} - \vec{V}_l \right\| \left( \left\| \vec{V}_{gas} - \vec{V}_l \right\| \right)} \quad (1)$$

where  $\rho$ ,  $V$  and  $D$  represented the density, velocity and diameters. The subscript ' $l$ ' and ' $gas$ ' signify the liquid and gas phase respectively.

Virepinte [1] proposed a correlation to take into account the interaction between droplets for single stream by introducing the spacing parameter  $C_o$  defined by  $C_o = S_l/D_l$ . Where  $S_l$  and  $D_l$  represent the distance between droplet and the droplet diameter respectively.

$$\frac{Cd}{Cd_{iso}} = 1 - 0.86e^{-0.053C_o} \quad (2)$$

The single droplet drag coefficient  $Cd_{iso}$  and Reynolds number  $Re$  are defined as:

$$Cd_{iso} = \frac{24}{Re} (1 + 0.12Re^{0.687}) \quad (3)$$

$$Re = \frac{\rho_{gas} D_l \left\| \vec{V}_{gas} - \vec{V}_l \right\|}{\mu_{gas}} \quad (4)$$

The object of this research is to examine an influence of droplet spacing not only from the front but also from lateral direction to approach the real sprays conditions. The drag coefficient is compared to the physical models available in the literature. The measuring techniques based on non-intrusive techniques are used to measure simultaneously the diameter, the velocity and the temperature of the droplets at different positions in the droplet stream.

## 2. Experimental setup

### 2.1. Droplet generator

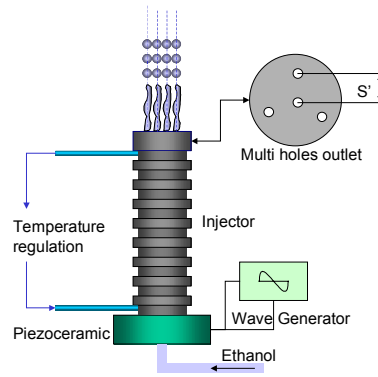


Figure 1 Injection system.

A monodispersed droplet generator[2] is based on a piezoceramic excited by a wave generator. The droplet characteristics can be modified by varying the frequency of the piezoceramic, injection pressure, changing the fuel physical properties and the injection temperature. Ethanol is used as the liquid fuel. The exit orifice is a thin diaphragm drilled

into 4 holes with 50  $\mu\text{m}$  inner diameters (Figure 1). The initial droplet diameter  $D_l$  is between 90 and 110  $\mu\text{m}$ . The droplet injection velocity is ranging from 2 m/s to 17 m/s.

### 3. Measuring techniques

In order to determine the drag coefficient, the droplet size  $D_l$ , the droplet velocity  $V_l$  and the droplet temperature  $T_l$  have to be measured along the droplet path. In fact, the droplet temperature is needed to determine the droplet physical properties (viscosity  $\mu_l$  and density  $\rho_l$ ). The gas phase velocity near the central stream is necessary for the drag calculation. A basic experiment based on smoke visualisation was also performed to obtain the gas phase velocity.

#### 3.1. Droplet diameter and temperature measurements

The measurements of size and temperature of the droplets are based on the droplet-light scattering technique. An argon laser beam is focused along the axis of the central droplet stream (Figure 2). The fringe scattering pattern can be observed in the forward direction.

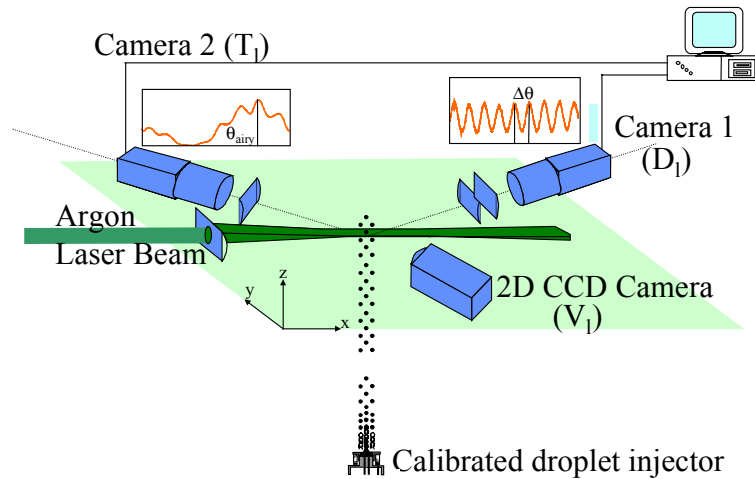


Figure 2 Measuring Technique Arrangement.

The equations of the geometrical optics can be used to calculate the intensity distribution of the forward scattered light. The prediction of the fringe pattern is independent on the gradient of refractive index inside the droplet for scattering angles  $\theta$  at  $30^\circ$  in the forward direction. The measurement of the angular interfering pattern  $\Delta\theta$ , for a forward scattering angle  $\theta$  allows to determine the droplet diameter following the relation:

$$D_l = \frac{2}{\Delta\theta \left( \cos\left(\frac{\theta}{2}\right) + n \sin\left(\frac{\theta}{2}\right) \right) \sqrt{1 - 2n \cos\frac{\theta}{2} + n^2}} \quad (5)$$

From this equation,  $n$  is the liquid refractive index. The forward-scattered fringe analysis can determine droplet sizing, without knowing the refractive index accurately (Eq. 5). The optical signal is recorded on a linear CCD camera on 2048 pixels and the auto correlation is calculated in order to eliminate the background noise. With this method, the determination of

the droplet size is done with an accuracy of 1.5%. Moreover, the relative size variation measurement accuracy is expected to be better.

A rainbow interferometry [3] is used to obtain the information of droplet temperature. The position of the first order bow observed in the backward diffusion is recorded by the second linear CCD array. The Airy/Walker theory [4] explains that the position of this rainbow  $\theta_{airy}$  is function of the liquid refractive index and droplet size:

$$\theta_{airy} = \theta_{rg} + \frac{1.0845}{\sin \tau_{rg}} \left( \frac{\lambda^2 \cos \tau_{rg}}{16 D_l^2} \right)^{1/3} \quad (6)$$

where  $\theta_{rg}$  is the position of the rainbow predicted from the geometrical optics theory:

$$\theta_{rg} = 2 \left[ 2 \arccos \left( \frac{1}{n} \sqrt{1 - \frac{n^2 - 1}{3}} \right) - \arcsin \left( \sqrt{\frac{n^2 - 1}{3}} \right) \right] \quad (7)$$

and

$$\sin \tau_{rg} = \sqrt{\frac{(n^2 - 1)}{3}} \quad (8)$$

The refractive index is linked to the droplet temperature by using a calibration curve obtained from the refractometry measurements. The uncertainty on the measurement is  $\Delta T = \pm 5^\circ \text{C}$ .

### 3.2. Droplet velocity measurement

The droplets are observed by shadowgraphy. The droplet spacing  $S_l$  determines the velocity when knowing droplet frequency  $f$ .

$$V_l = S_l \times f \quad (9)$$

The maximum error obtained from this measurement is 1.5%.

By simultaneously measuring the droplet size, velocity and temperature at different locations downstream from the injector, the temporal evolution of the liquid phase can be determined.

### 3.3. Gas phase velocity measurement

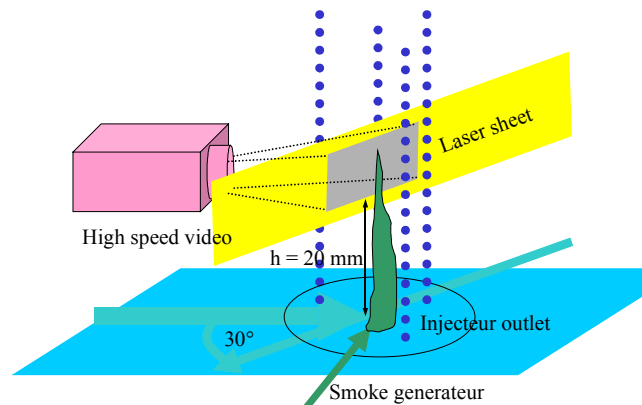


Figure 3 Smoke Generator and Visualisation Apparatus Arrangement.

A silicon smoke generator outlet is located perpendicularly to the section of the injector. The smoke velocity at the outlet is 0.5 m/s. The argon laser sheet, with a thickness less than 100 $\mu$ m, is closed and parallel to the central jet (Figure 3). A high speed video camera is used to observe the smoke front and to determine the velocity of entrained gas phase near the central droplet stream. The smoke front is followed between 20-30 mm from the injector outlet corresponding to the droplet velocity measurements zone. By determining the evolution of smoke front, we obtained the mean velocity of gas phase near the central droplet.

## 4. Results and Discussion

### 4.1. Gas phase velocity

The tests have been performed with the different diaphragm configurations. A large range of lateral distance parameters  $C'$  ( $C'=S'/D_j$ ) is explored, between 4 to 26.

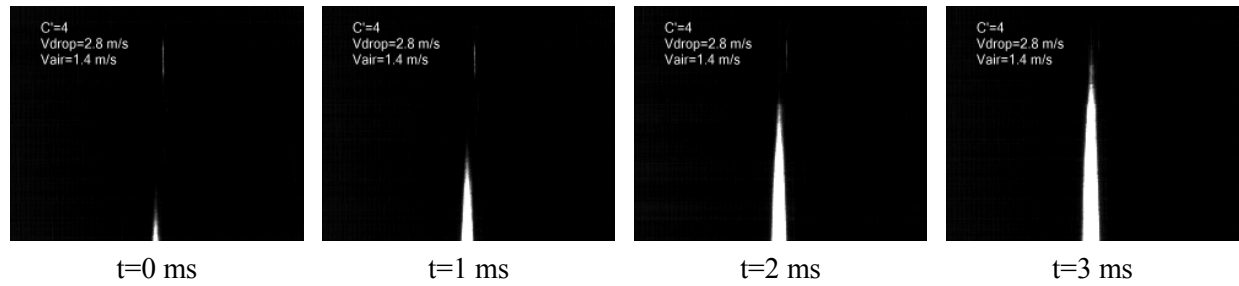


Figure 4 Smoke front displacement observed from high speed camera 2 kHz (case:  $C'=4$ ,  $Re=21$ ).

By using the silicon smoke as a tracer and an Argon laser sheet lighting near the central stream, the velocity of gas phase can be identified. The observation of the flow was performed with a high speed video camera. Figure 4 shows the temporal evolution of the smoke front around the central jet stream. A number of sequences was analysed in each experimental configuration to determine the gas phase mean velocity.

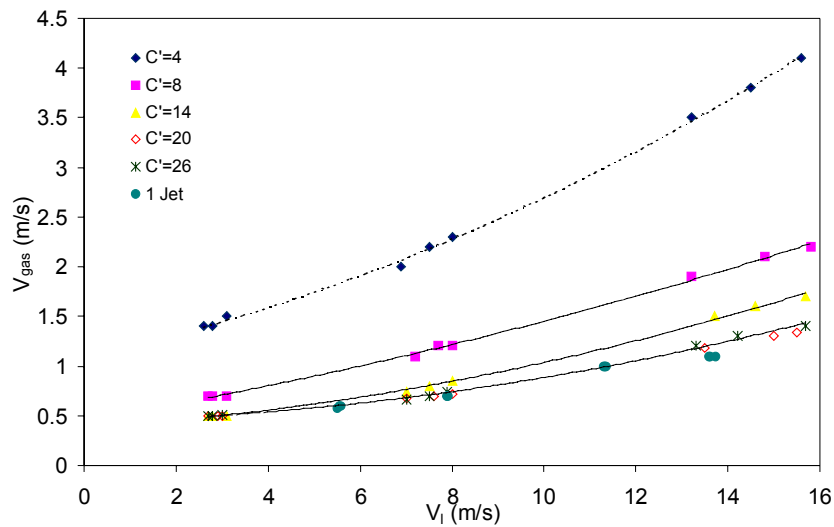


Figure 5 Gas phase velocity of central jet, influence of adjacent jets.

Figure 5 shows the gas phase velocity evolution closed to the central stream. These velocities depend on the droplet velocity and the non-dimensional lateral distance between droplets  $C'$ . For the central stream, the range of initial vertical distance between droplets  $C_o$  is 2.6 to 3.5 times of the droplets diameter. In this range of droplet spacing for the central jet, the gas aspiration is considered to be constant. The result shows the influence of lateral distance between jets on the entrained gas phase velocity around the central jet. For closed lateral jets, the gas velocity increases substantially. However, this influence is neglected for the lateral distance parameter larger than 20 which gives the same result as isolated jet.

#### 4.2. Droplet drag coefficient

The results can be divided in two regimes : low and high lateral interaction. For low lateral interaction ( $8 < C' < 26$ ) the effect of lateral droplet spacing on the drag coefficient can be neglected in comparison to the influence of the wake generated from the upstream droplets.

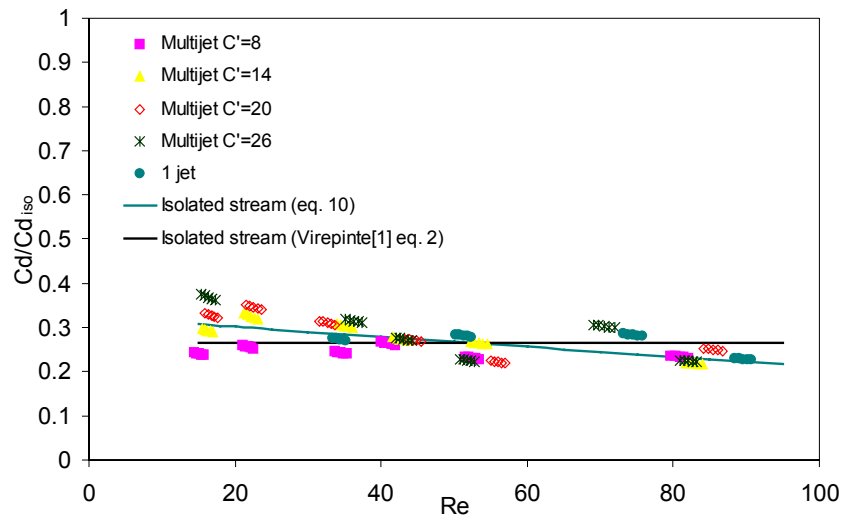


Figure 6 Droplet drag coefficient normalized by isolated droplet drag coefficient ( $Co=3$ ).

The results are in agreement with an isolated stream case. However, these results show the slope decreasing with the Reynolds number due to the influence of entrained air around the droplet stream. The experimental results are fitted with a linear equation as shown in Figure 6 to obtain a new correlation giving the evolution of droplet drag coefficient in a convective flow.

$$\frac{Cd}{Cd_{iso}} = -0.001145Re + 1.21913589(1 - 0.86e^{-0.053Co}) \quad (10)$$

The isolated droplet drag coefficient  $Cd_{iso}$  is given from expression (3). The previous relation is valid in the case of an isolated droplet stream for the following conditions :  $Co$  closed to 3 and  $15 < Re < 95$ .

For the high lateral interaction, at low Reynolds number, the effect of interaction from the neighbouring droplets induces a reduction of the droplet drag coefficient in comparison with the isolated stream case as shown in Figure 7. When the Reynolds numbers is larger than 45, the multidroplet interaction causes a rapid increase of the drag coefficient. The values of the drag coefficient are very sensitive to the wake angle generated from the neighborhood droplets.

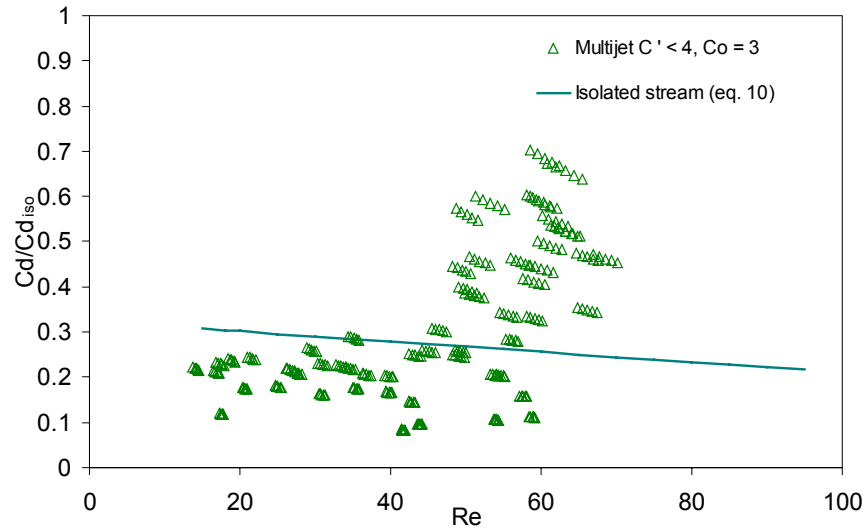


Figure 7 Droplet drag coefficient correction term under high lateral interaction.

Silverman et al.[5] studied numerically the interaction effect of neighboring droplets in dense spray and reviewed that the effects of the neighboring side-by-side droplets, at very small distances, cause an increase of drag coefficient. As can be seen, the drag coefficient ratio can become higher than unity if the droplets are very close (i.e. the drag coefficient of a highly interacting droplets is higher than isolated droplet one). The effect of the azimuthal wake angles generated from the neighboring droplets is also presented.

These experimental results are compared with numerical results of Silverman shown in Figure 8 (a). The experimental transition zone corresponding to a rapid inversion of the slope of the curve for a droplet distance  $C'$  about 3 is in a good agreement with the numerical results.

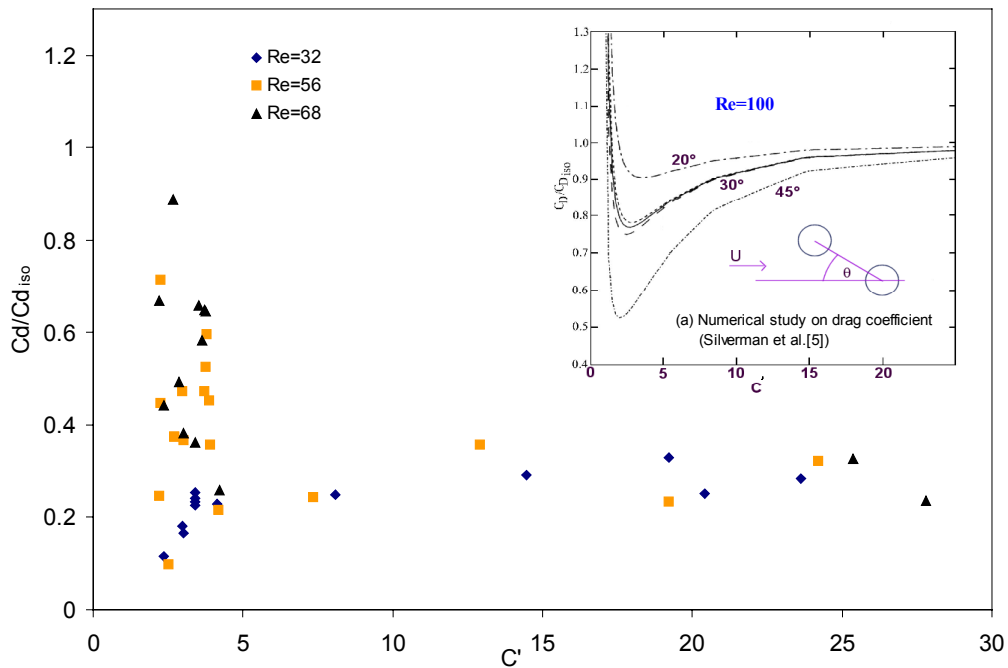


Figure 8 The effect of lateral distance on the drag coefficient.

However, for the experimental approach the droplets are always under the wake generated from upstream droplets. Without the influence of interaction of the side-by-side neighboring droplets, the drag coefficient is always equivalent to the isolated jet stream configuration (Figure 8).

## 5. Conclusion

The droplet drag can vary widely depending not only on the Reynolds number but also on the geometrical arrangement of neighbours droplets. The droplet drag coefficient decreases for low spacing parameter in the case of one stream. At low Reynolds number ( $Re < 45$ ), It has been found that this decreasing is higher when the droplets travel in tandem (several adjacent jets). For Reynolds numbers around 45 a transition appears corresponding to a high dispersion of the drag coefficient values. This dispersion should be considered as the effect of the geometry of neighbouring droplets and the wake angle. For higher Reynolds numbers and low lateral distances, the drag coefficient increases very rapidly and can be greater than the isolated droplet one. This tendency is in good agreement with numerical results performed by Silverman [5].

The objective of this study is to improve the numerical simulation of dense sprays by taking into account the influence of droplets interaction. The results presented before concern simple arrangements of monosized droplet streams. To validate these results a new experiment will be performed in a confined configuration with a well known gas phase velocity profiles (mean and fluctuating velocities). A high droplet concentration will be injected in this flow to study the evolution of droplet velocity and to evaluate the drag coefficient in the case of a turbulent two phase flows.

The study is now oriented under the reacting conditions. This study will give more comprehension on the droplets interaction inside the combustion chamber. The experimental results shows the decreasing of drag coefficient and the burning rate for low distance between the stream.

## 6. References

- [1] Virepinte, J.F., Etude du comportement dynamique et thermique de gouttes en régime d'interaction dans le cas de jets rectilignes, PhD thesis, Ecole Nationale Supérieure de l'aéronautique et de l'Espace (1999).
- [2] König, G., Anders, K., Frohn, A., A new light-scattering technique to measure the droplet diameter of periodically generated moving droplets, Journal of Aerosol Science, Vol.17, n°29, 429-437 (2000)
- [3] J.P.A.J. Van Beeck, M.L. Riethmuller, Rainbow interferometry with wire diffraction for simultaneous measurement of droplet temperature, size and velocity, Part. Part. Syst. Charact., vol. 14, p.186-192, 1997.
- [4] Walker, J.D., Rainbows from single drops of water and other liquids, Am. J. Phys., 44(5), 421-433 (1976).
- [5] Silverman, I. and Sirignano, W.A., Multidroplet interaction effects in dense sprays, Int. J. multiphase flow, vol. 20, n°1, 99-116 (1994).